JOURNAL OF THERMOPHYSICS AND HEAT TRANSFER
Vol. 15, No. 2, April–June 2001

Entry Conditions in Planetary Atmospheres: Emission Spectroscopy of Molecular Plasma Arcjets

V. Lago,* A. Lebéhot,* and M. Dudeck†
Centre National de la Recherche Scientifique, 45071 Orléans, France
S. Pellerin‡
Centre Universitaire de Bourges, 18028 Bourges, France
T. Renault§
Université de Limoges, 87060 Limoges, France
and
P. Echegut¶
Centre de Recherche sur les Matériaux à Haute Température,
Centre National de la Recherche Scientifique, 45071 Orléans, France

A stationary arcjet, operating at low pressure (0.13 mbar in the vacuum chamber), is used for the simulation of the gas flow surrounding a vehicle during its entry into the atmosphere of Titan and Mars. For the Titan atmosphere the gas mixture 99% N_2 − 1% CH_4 is used and 97% CO_2 − 3% N_2 for the Martian atmosphere. The respective plasma arcjets are analyzed by optical emission spectroscopy for identifying the emitting molecules and atoms and also deducing the temperatures associated with their different internal modes. For the N_2–CH_4 plasma the vibrational temperatures T_v deduced from CN and NH spectra are found in concordance with the measured electron temperature, that is, 8000 K, whereas, from CH spectra, T_v is obtained close to 3700 K. The rotational temperatures are found to be between 2500 and 2800 K for CH and NH and nearly 5000 K for both CN and N_2^+ spectra. For the CO_2–N_2 plasma no emission from the arcjet is detected in the UV–visible range; the feasibility of the infrared analysis of the $\Delta v = 2$ band of CO is demonstrated in a stationary plasma discharge experiment.

Nomenclature

B_e	=	rotational constant
c	=	velocity of light
F	=	rotational energy
h	=	Planck constant
I	=	intensity of line
k	=	Boltzmann constant
L	=	axial distance from the nozzle exit
N	=	angular momentum of nuclear rotation
S	=	square of the dipolar transition element for rotation
T_r	=	rotational temperature
T_v	=	vibrational temperature
t	=	time
v	=	vibrational quantum number
Λ	=	component of the electronic orbital angular momentum along the internuclear axis
λ	=	wavelength

I. Introduction

PLASMA arcjets are often considered as important tools in space technology. They are studied as thrusters for spacecrafts[1–3] and also for the simulation of space conditions, for instance, during the entry process into a planetary atmosphere.[4,5] In the actual planetary entry conditions a shock wave appears in front of the space probe, and a plasma is generated by the local heating of the atmosphere produced by this shock wave. Between the shock wave and the probe surface, a relaxation of the plasma properties occurs until the surface is reached. The properties of interest are generally those that are achieved at the surface for the study of the wall heating and erosion.

Therefore, in laboratory simulation it is important to get a complete knowledge of the properties of the plasma jets, theoretically[3,6,7] as well as experimentally.[8–11] In the ground test facilities of Laboratoire d'Aérothermique, the properties of the space environment surrounding a vehicle can be simulated for the entry conditions into a given atmosphere.[5]

The present work is an investigation of emission spectroscopy with two different plasma flows (N_2–CH_4 and CO_2–N_2) for the simulation of Titan and Mars atmospheres.

II. Experiment

The present measurements were carried out with the plasma wind tunnel SR1 (length 3.4 m, diameter 1 m), where a dc arc jet generator (Fig. 1) is operated for the production of stationary plasma flows.

The arc discharge is generated between the tip of a cathode, which is a small zirconium disk inserted into copper (disk diameter 1.6 mm), and the nozzle throat, which operates as the anode (cylindrical neck of 4 mm length and 4 mm internal diameter, made of tungsten inserted into copper). Copper pieces, anode as well as cathode, are water cooled. The exit diameter of the diverging part of the anode is 48 mm. With a vortex-stabilized arc at low currents (50–200 A) and low mass-flow rates (0.1–0.3 g s^{-1}), continuous plasma jets are obtained in steady conditions. The average specific enthalpy ranges from 5 to 22 MJ kg^{-1}. Roots pumps (with a pumping speed of 24,000 m^3 h^{-1}) allow an ambient pressure of 0.13 mbar to be maintained in the vacuum chamber during operation of the arc jet.

For the simulation of the entry conditions into the Titan atmosphere, the gas mixture (99% N_2 and 1% CH_4) is prepared by introducing a mass-flow rate of 0.258 g s^{-1} for N_2 and 0.005 g s^{-1} for CH_4. Thus, the amount of CH_4 corresponds to the smallest value

Received 27 September 1999; revision received 2 November 2000; accepted for publication 6 November 2000.

*Research Scientist, Laboratoire d'Aérothermique, 1C Avenue de la Recherche Scientifique.
†Professor, Laboratoire d'Aérothermique and Université Pierre et Marie Curie, Place Jussieu, 75252 Paris Cedex 5, France. Member AIAA.
‡Research Scientist, LASEP, Rue Gaston Berger, BP 4043.
§Research Scientist, Faculté des Sciences, 123 Avenue Albert Thomas.
¶Research Scientist, 1D Avenue de la Recherche Scientifique.

expected for the Titan atmosphere. In the case of the Martian atmosphere, a mixture of 97% CO_2 and 3% N_2 is used, with the respective mass-flow rates 0.249 g s^{-1} and 0.0014 g s^{-1}. In these conditions the average specific enthalpy is about 10.9 MJ kg^{-1} for the CO_2–N_2 plasma and 8.2 MJ kg^{-1} for the N_2–CH_4 plasma.

Air plasmas can be maintained with steady conditions during several hours (about 8 h of continuous run); this operating time is limited mainly by the lifetime of the zirconium tip of the cathode. Adding a carbonated compound (such as CO_2 and CH_4) in the plasma decreases its lifetime significantly. In these conditions it can be observed that all of the water-cooled surfaces inside the vacuum chamber are polluted with a black layer of carbon or carbonic soot within a few minutes. The pollution of the anode leads to an unstable behavior of the arc and accelerates the erosion of the zirconium tip. Then, the operation time is limited to about two hours. Because the quartz window for the optical emission is not water cooled, it remains free from any deposition.

The plasma parameters in the plume can be analyzed locally by moving the plasma generator along the horizontal and vertical axis. The displacement ranges are 65 cm along the plasma jet axis and 40 cm perpendicularly.

For the CO_2 plasma two different experiments are performed. At first, the Martian atmosphere is studied at Laboratoire d'Aérothermique with the working conditions just described, and the spontaneous emission of the plasma is analyzed in the near UV and visible domains (275–900 nm). Another experiment is performed in CRMHT Laboratory for very different plasma conditions and a different wavelength range for the analysis. This second experiment is a small plasma source located in a cylindrical chamber (40 cm in length, 10 cm in diameter) equipped with two CaF_2 windows for the optical measurements (Fig. 2). A Fourier transform infrared (IR) spectrometer allows the CO_2 plasma to be analyzed in the IR wavelength region. The working gas (pure CO_2) is introduced axially, the mass flow is controlled, and a primary pump maintains an atmospheric pressure in the chamber. The arc discharge is sustained between two cylindrical electrodes with a conical tip made of tungsten (summit angle 60 deg). The distance between the electrode tips can be adjusted using an insulated micrometric screw. The arc is ignited by shortening the distance between the electrodes (typically to 5 mm); in steady regime an arc of 10 mm length is maintained using a high-voltage ac electric supply (10 kV, 150 mA, 50 Hz).

Such a plasma source does not simulate properly the conditions of planetary reentry, but is a first step for this study. The main goal here is to detect the CO emission in the IR range and to perfect the simulation of the $\Delta v = 2$ band of the CO spectrum from the comparison with an experimental spectrum.

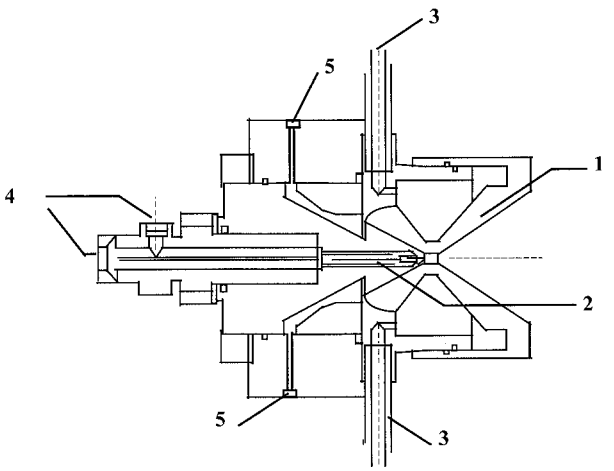

Fig. 1 Schematic of the arcjet generator: 1, anode; 2, cathode; 3, anode water-cooling circuit; 4, cathode water-cooling circuit; and 5, gas injection.

III. Optical Emission Spectroscopy

Thanks to the intense radiation that is emitted by the plasma jet, a number of physical parameters can be determined through the analysis of the light emitted spontaneously by means of optical emission spectroscopy, which has the advantage to be a nonintrusive diagnostics tool.[8,9] Rotational and vibrational spectra can be observed, and some plasma parameters, such as the rotational and vibrational temperatures, T_r and T_v, respectively, can be deduced. Therefore a high-wavelength resolution is needed for resolving the rotational lines.

A. UV–Visible Experimental Setup

The experimental setup for the measurements in the near UV and visible wavelength range is shown in Fig. 3. The monochromator (SOPRA F1500, Ebert–Fastie type) has a focal length of 1500 mm and a grating of 1800 grooves/mm. The plasma is imaged onto the monochromator by a mirror telescope connected to the entrance slit by a quartz optical fiber. The detector is an intensified optical multichannel analyzer (OMA, Princeton Instruments IRY 1024). This device allows an 8.5-nm wavelength region to be expanded on 1024 pixels. The OMA is cooled by a Peltier element, which gives an operating temperature of −35°C.

Although the plasma column has a good cylindrical symmetry, no Abel inversion is performed (except when especially mentioned), and the radiation collected by the spectrometer is the result of an integration along a diameter of the arcjet, on the jet axis, at a given distance L from the nozzle exit. Then, it must be noticed that the properties deduced from the corresponding spectra are averaged over this diameter. This means that, for deducing vibrational or rotational temperatures from the recorded spectra, it must be assumed that the different corresponding state populations are distributed with the same relative radial profile at a given distance from the nozzle exit.

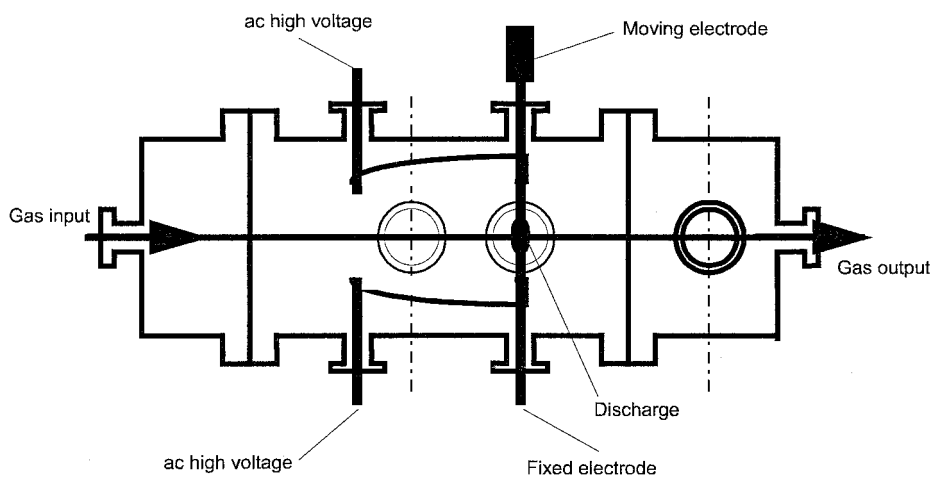

Fig. 2 Experimental setup for the CO spectrum study in the IR wavelength range.

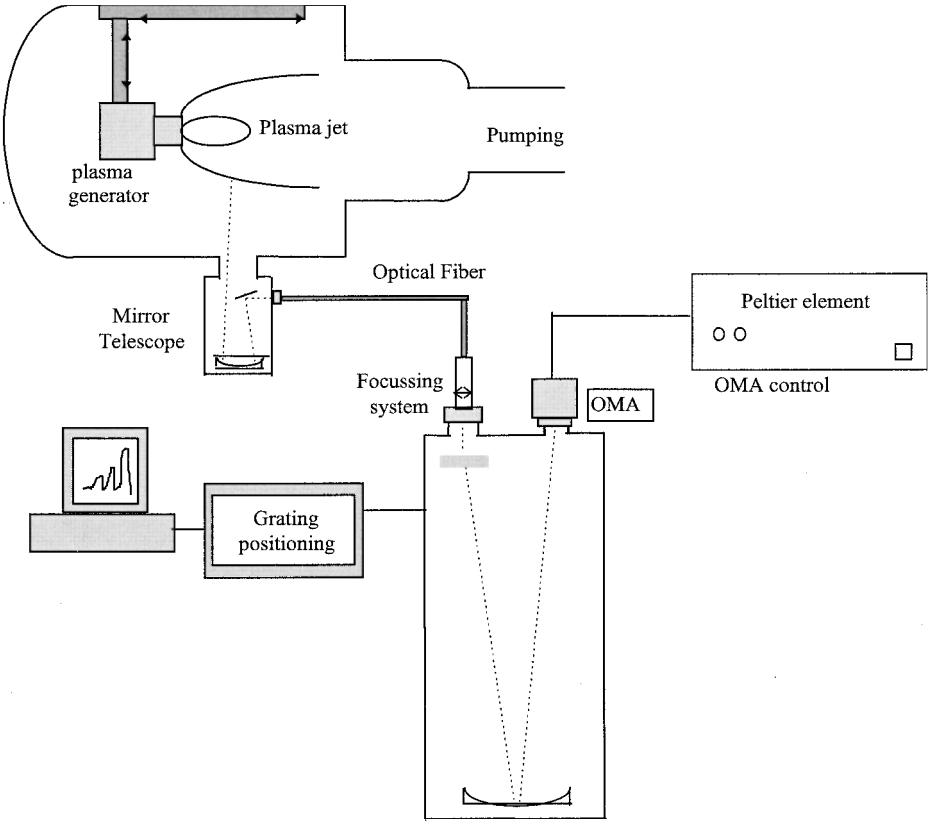

Fig. 3 Optical setup for the near UV and visible wavelength range.

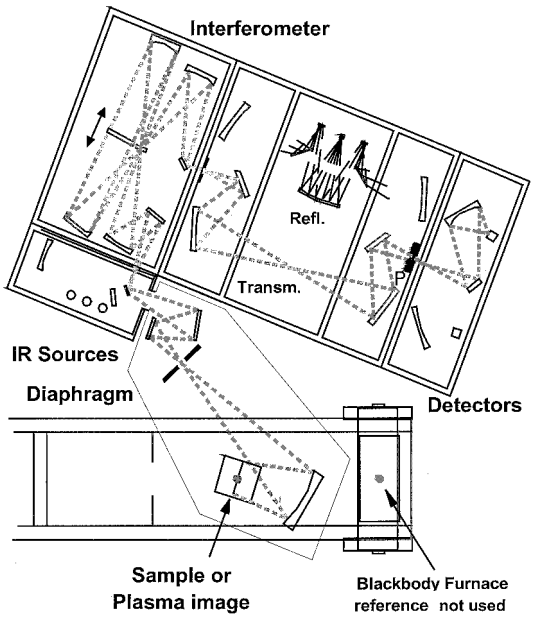

Fig. 4 Schematic of the FTIR spectrometer (CRMHT-CNRS Orléans, France).

B. IR Experimental Setup

The experimental setup employed for the IR analysis is a Fourier transform IR (FTIR) spectrometer (Bruker IFS 113v). Figure 4 shows the scheme of the apparatus. The FTIR principle is based on the Michelson interferometer. The incident radiation (the flux emitted by the plasma discharge) is split into two beams reflected by a mobile mirror. Each one follows a different optical path. They are combined again after following these different ways. The mirror motion induces that one part of the analyzed beam is ahead of the other by a time Δt. The detection is performed by an InSb (indium antimonide) detector, and the calculator transforms the time-depending signal into the spectrum (intensity vs wavelength). This spectrometer is working for reflection and transmission on solid surfaces. A home-made device is coupled to the spectrometer for measuring the spectral emissivity of solids and molten materials. To analyze the light emitted from the plasma discharge, the arc image is focused onto the usual sample spot, and the light emitted by the plasma is then introduced into the spectrometer via a flat mirror.

C. Molecular Diagnostic Method

The rotational (T_r) and/or vibrational (T_v) temperatures can be deduced through molecular emission spectroscopy, even if the emission spectra are noisy and not completely resolved, regarding the wavelength structure, caused by the limited wavelength spread $\Delta\lambda_{app}$ (apparatus function) delivered by the complete analysis device. The method described next is based on a numerical comparison of the experimental spectrum with a corresponding theoretical spectrum. It can be applied in the temperature range 300–10,000 K.

The following procedure is applied. First, the measured spectrum is corrected for the continuous background, which is generally assumed to be linear in the spectral range of interest. The experimental spectrum is normalized to the head band peak intensity, and the apparatus function $\Delta\lambda_{app}$ is estimated from the profile of an isolated line in the spectrum, or from the shape of the band head.[12,13] Then, a rather good estimation of temperatures can be made quickly by a simple comparison of the theoretical and experimental intensities of two selected components of the spectrum. The uncertainty on the resulting temperature is related to the precise identification of these components, to the sensitivity of the corresponding intensity ratio to the temperature, and to the choice of the continuous background level. The best choice of such a thermometer test function should be made with respect to the analysis of possible systematic errors. For example, adequate test functions for OH, C_2, and CH are published in previous publications (see for example Refs. 12–15). If the synthetic spectrum describes correctly the wavelength location of the rotational and vibrational lines, it is also possible to compare point by

point the experimental data with the simulated spectrum. Then, a numerical minimization procedure, initiated using a test function, can be used in order to minimize the mean square variation as a function of the temperatures T_r and T_v and of the apparatus function $\Delta\lambda_{app}$.

If a well-resolved molecular spectrum can be obtained, the numerical superposition procedure can be initialized using the temperature values deduced from the Boltzmann plot given by the measured line intensities. If most of neighboring spectral lines are overlapping, the Boltzmann plot method cannot be used.

IV. N_2–CH_4 Plasma

With the arcjet experiment several bands of the emission spectrum are intense enough for being used in the determination of rotational and/or vibrational T_v temperatures. Because these bands partially overlap, only some wavelength intervals of the spectral region are fit for use. Here, special attention is devoted to the CH ($A^2\Pi \rightarrow X^2\Sigma$) transition and to the CN violet bands, as well as to the N_2^+ ($B^2\Sigma \rightarrow X^2\Sigma$) first positive system and the NH ($A^3\Pi \rightarrow X^3\Sigma$) electronic transition. The aim is to deduce from these spectra the rotational and vibrational temperatures for the electronic ground state of the respective neutral species. For this purpose the emission spectra are simulated from the ground state populations, assuming that the upper electronic level is excited only by electron impact. Then, the vibrational population of the upper level is the result of the ground state distribution multiplied by the appropriate Franck–Condon factors. For the rotational population it is assumed to be the same for the upper level and for the ground state. The deexcitation is considered to be fully radiative. Therefore, with these assumptions[15] an emission spectrum reflects the ground state rotational and vibrational distributions. This model is justified because, under the present plasma conditions, for all of the molecules of interest the radiative decay frequencies are greater than the collision frequencies.

A. CH ($A^2\Delta \rightarrow X^2\Sigma$) Spectrum

The approach presented by Koulidiati[16] for the $\Delta v = 0$ systems around 430 nm is used for the simulation of the CH molecular band. The energy levels are described in intermediate coupling, and the Λ doubling is taken into account only for the $^2\Pi$ state. Then, the high molecular vibrations are described using a supplementary term obtained from the experimental data of Fagerholm.[16] Nevertheless, the global simulation of the spectrum for the determination of the rotational and vibrational temperatures is not the proper way because of the perturbations of the CH spectrum arising from the emission of other emitting molecules in the same wavelength region. Therefore, thermometric lines of CH are chosen in the R branch, which can be used to deduce a rotational temperature from test functions. These thermometric lines are well isolated and not perturbed. Such four lines are listed in Table 1. The intensities of these four lines (and only them) are here treated by the inverse Abel transform in order to obtain the local corresponding population densities. The rotational temperature T_r to be determined is then connected to the relative corrected intensities through the Boltzmann law:

$$\ln\left(\frac{I^{N',v'}_{N'',v''}}{S_{N',N''}}\right) = -\frac{hcF(N')}{kT_r}$$

where I is the intensity of the line (after Abel transform, and expressed as a number of photons per time unit), corresponding to the transition (N', $v' \rightarrow N''$, v''), and $F(N')$ is the rotational energy

Table 1 Thermometric lines chosen for the CH molecule

No.	Line	Vibrational band	Wavelength, nm
1	R1cd (19)	(0,0)	419.316
2	R1cd (16)	(0,0)	421.218
3	R2cd (14)	(0,0)	422.603
4	R1cd (13)	(0,0)	423.106

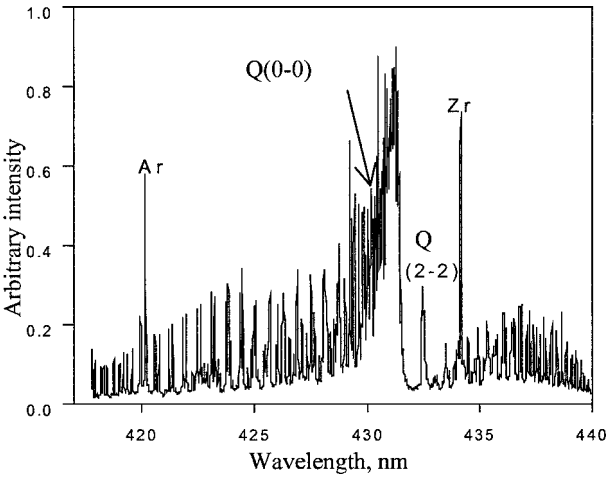

Fig. 5a Experimental spectrum for CH in the 415.0–440.0 nm wavelength range with the mixture N_2 (99%)/CH_4 (1%); distance from the nozzle exit: $L = 1$ cm.

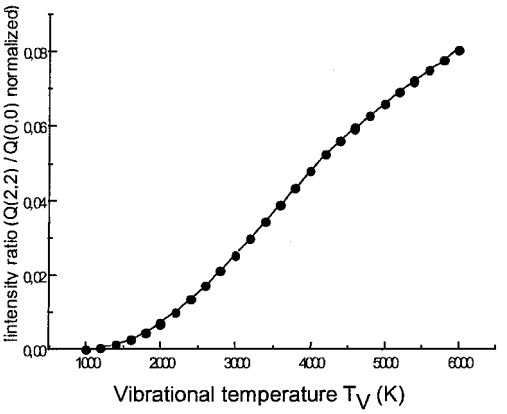

Fig. 5b Vibrational temperature determination from the ratio between the Q(2-2) and the Q(0-0) simulated intensities.

of level N'. The local rotational temperature is then evaluated. It appears that the relative intensities of the three branches P, R, and Q of the theoretical spectrum depend strongly on the vibrational and rotational temperatures. The Q(2,2) band head is well isolated, and the ratio of its maximum to the maximum of the merged Q(0,0) and Q(1,1) band heads varies with vibrational temperature, but not with rotational temperature. Thus, the Q(2,2) band head can be used for the evaluation of the vibrational temperature.[14,16]

An example of experimental spectrum is given in Fig. 5a. The CN violet band is also present; as just mentioned, this prevents the global simulation method to be applied successfully. The determination of the rotational temperature requires successively: 1) the transverse measurement of the intensity of the four thermometric lines; 2) the calculation of the inverse Abel transform in order to work in the axial symmetry; 3) the extraction of the populations corresponding to the emitting states of the four lines and their presentation in a Boltzmann plot. Applying this method leads to an axial rotational temperature of 2500 K for the conditions of Fig. 5a. For the calculation of the vibrational temperature, the ratio of the Q(0,0) maximum to the Q(22) maximum is calculated for a rotational temperature of 2500 K, as just determined, vs the vibrational temperature. This test function is reported in Fig. 5b. The vibrational temperature corresponds to the point where the ratio is the same as the experimental value. The spectrum of Fig. 5a gives then a vibrational temperature of 3700 K.

B. CN ($B^2\Sigma \rightarrow X^2\Sigma$) Violet System Around 388.5 nm

The CN violet system is observed as the transition CN ($B^2\Sigma$, v′ $\rightarrow$ $X^2\Sigma$, v″). Two bands are clearly observed under the

present plasma conditions: the $\Delta v = 0$ diagonal band and the $\Delta v = -1$ band.

For the CN violet system it is not possible to resolve individual spectral lines for determining a rotational or a vibrational temperature. Lines from the (0-0) and (0-1) rotational bands are lying too close to each other to be resolved, and lines from other vibrational transitions are all overlapping with each other. Therefore, in the case of CN, the complete interpretation of the spectrum is based on the overall comparative method. Several sets of molecular data are tested,[17–20] and the best agreement is found with the vibrational and rotational constants given by Ito et al.[20] These constants also give the best agreement for the wavelength location of the spectral lines. However, the measured intensity distributions are not accurately reproduced. Then, the vibrational temperature is obtained through the best global agreement between the measured and simulated spectra. The rotational temperature is preferably determined from a best fit of the rotational lines of the (0-0) transition. For both vibrational and rotational temperatures the error is expected to be lower than 500 K, as far as the molecular constants are correct. This extent of error is only evaluated from the comparison between calculated and recorded spectra; this is rather a statistical error on the treatment procedure than an actual experimental accuracy. An example of experimental and simulated spectra for the diagonal bands measured at a distance $L = 2$ cm from the nozzle exit is shown in Fig. 6. The temperatures obtained are close to $T_v = 8000$ K for vibration and $T_r = 5000$ K for rotation, with the apparatus function $\Delta\lambda_{app} \approx 0.022$ nm.

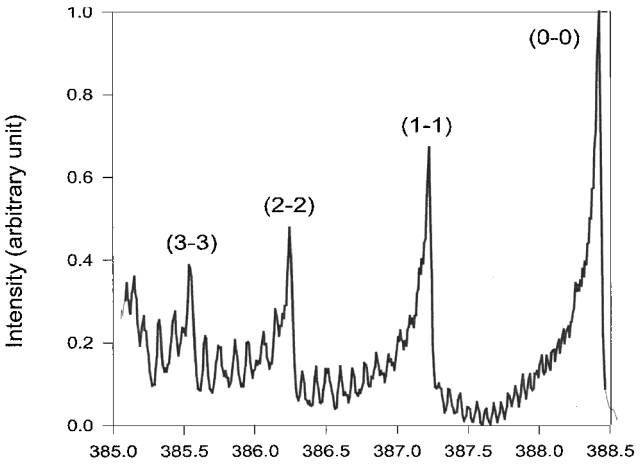

Experimental spectrum

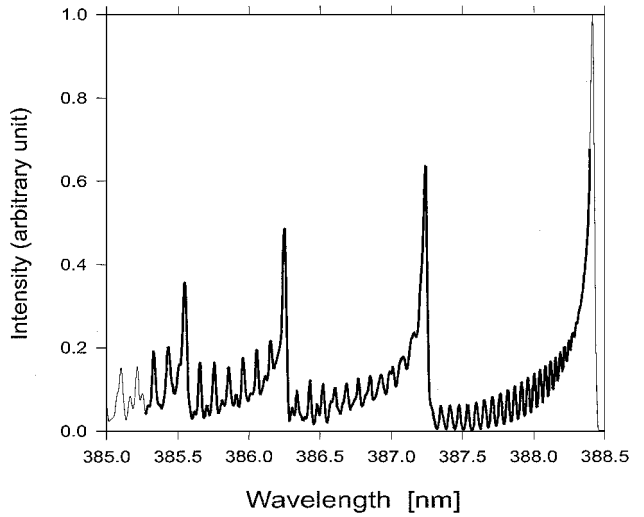

Simulated spectrum

Fig. 6 Spectra for CN in the 385–388.5 nm wavelength range in the same conditions as in Fig. 5. The simulated spectrum is calculated with the temperatures T_v = 8000 K and T_r = 5000 K.

C. NH ($A^3\Pi \rightarrow X^2\Sigma$) Transition Around 336.0 nm

The emission is observed for the transition NH ($A^3\Pi \rightarrow X^2\Sigma$). Only the (0-0) and (1-1) vibrational bands can be observed with a reasonable signal-to- noise ratio. The spectrum is simulated with the molecular constants taken from Brazier et al.[21] These constants are not accurate enough for reproducing the wavelengths of most of the rotational lines within the limits of the apparatus resolution. However, the agreement is still better than with the constants taken from Huber and Herzberg,[18] and, for rotational levels up to 20, the overall structure looks very similar to the experimental spectrum. For higher rotational levels the experimental spectrum always exceeds the simulated intensities. This point will be discussed in Sec. IV.E. An example of measured and simulated NH spectrum is shown in Fig. 7. The rotational temperature is determined from lines corresponding to rotational levels up to 20 and are well resolved. Then the vibrational temperature is determined with the ratio between the two band heads (0-0) and (1-1). The temperatures are found to be $T_v = 8000$ K for vibration and $T_r = 2800$ K for rotation (with $\Delta\lambda_{app} \approx 0.020$ nm) at a distance $L = 1$ cm from the nozzle exit.

D. N_2^+ ($B^2\Sigma \rightarrow X^2\Sigma$) First Negative System Around 391.4 nm

The first negative system of the molecular ion of nitrogen corresponds to the transition $N_2^+(B^2\Sigma_u^+) \rightarrow N_2^+(X^2\Sigma_g^+)$. A good agreement for the intensities as well as for the wavelengths of the spectral lines is obtained, with the vibrational and rotational constants taken from Krupenie and Lofthus.[22] For the rotational temperature the accuracy is better than 500 K. The determination of the vibrational temperature is more hazardous because the intensity of the spectrum

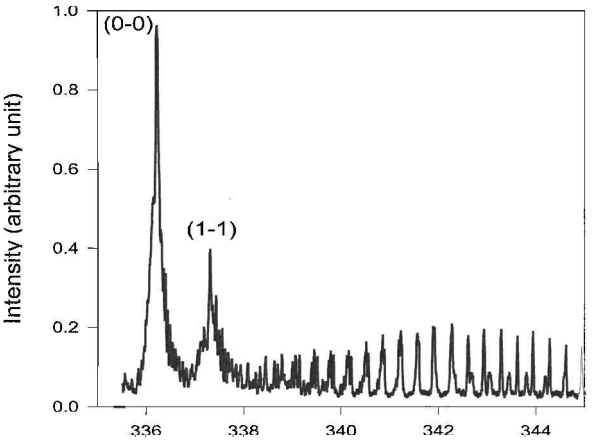

Experimental spectrum

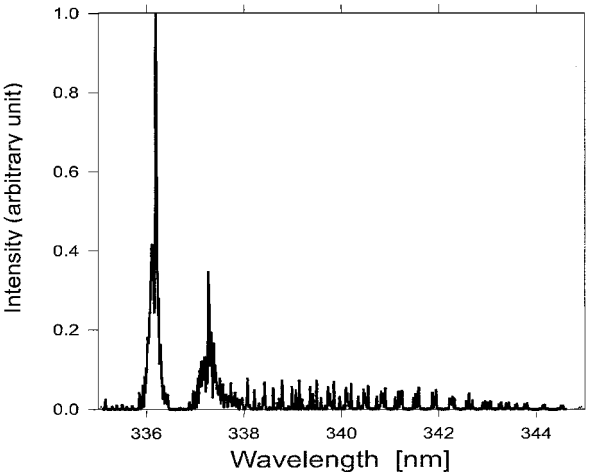

Simulated spectrum

Fig. 7 Spectra for NH in the 335–345 nm wavelength range in the same conditions as in Fig. 5. The simulated spectrum is calculated with the temperatures T_v = 8000 K and T_r = 2800 K.

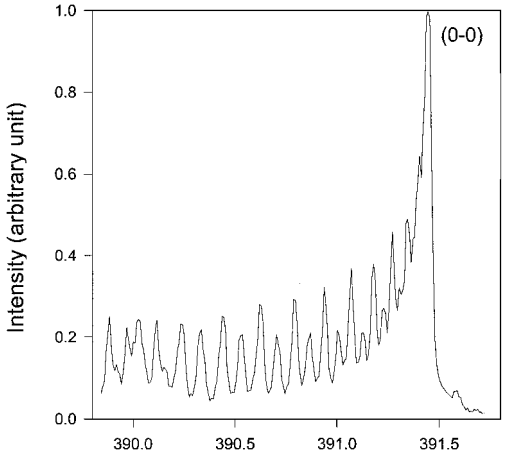

Experimental spectrum

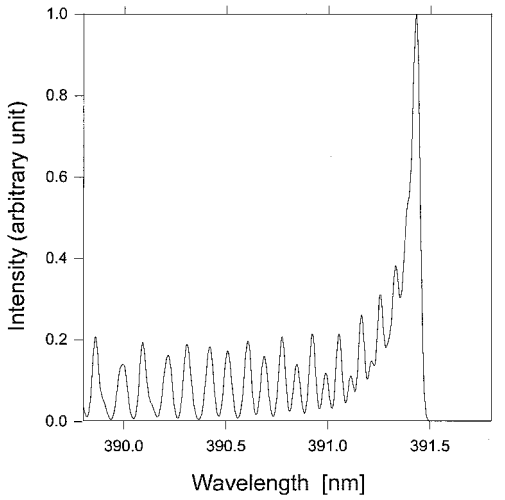

Simulated spectrum

Fig. 8 Spectra for the N_2^+ first negative system in the 389.8–391.8 nm wavelength range in the same conditions as in Fig. 5. The simulated spectrum is calculated with the temperature $T_r = 2200$ K.

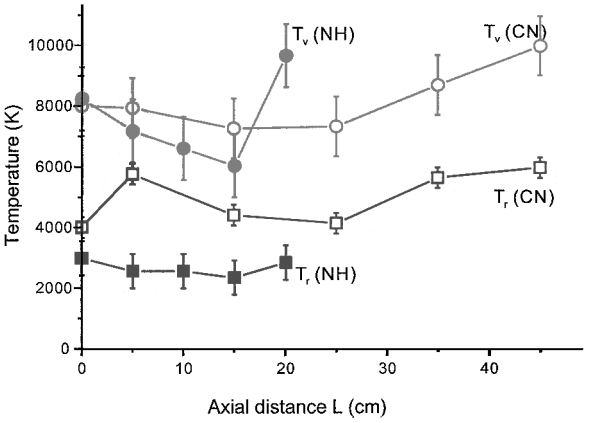

Fig. 9 Rotational temperature (T_r, □, ■) and vibrational temperature (T_v, ○, ●) for NH (●, ■) and CN (○, □) as a function of the distance L from the nozzle exit, for the mixture N_2 (99%)/CH_4 (1%).

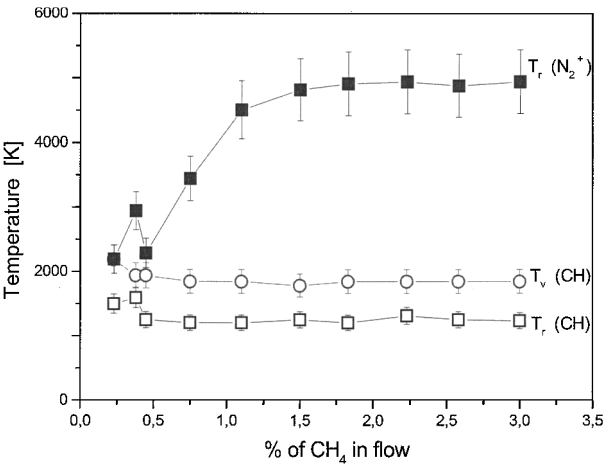

Fig. 10 Rotational (□, ■) and vibrational (○) temperatures for N_2^+ (■) and CH (□, ○) as a function of the methane percentage in the N_2/CH_4 flow for the distance $L = 2$ cm from the nozzle exit.

corresponding to the (1-1) band is weak compared with the intensity of the (0-0) band. Because of overlapping, the intensities of the (1-1) band can only be determined with a poor accuracy. Examples of measured and simulated spectra, taken at a distance $L = 1$ cm from the nozzle exit, are given in Fig. 8. The rotational temperature thus obtained is close to $T_r = 2200$ K, with the apparatus function $\Delta\lambda_{app} \approx 0.034$ nm. The agreement between the experimental and simulated spectra is quite satisfactory, except for wavelengths lower than 390.5 nm where the intensity alternation is not quite fitted.

E. Discussion of the Results for the N_2–CH_4 Plasma

Figure 9 shows the rotational and vibrational temperatures along the plasma plume axis, as determined from the NH spectrum. The distance from the nozzle exit ranges here between 0 and 200 mm. At larger distances the intensity of the emitted light becomes too weak. The rotational temperature over this distance range is nearly constant, at 2800 ± 300 K. If the upper rotational levels are considered (>20), a substantial overpopulation is noticed, with respect to the Boltzmann equilibrium distribution; this could be an effect of the radial distribution of the rotational temperature in the arcjet, with colder parts on the outer edge of the jet. Then, the measurements appear as an average along a diameter of the jet, and the integrated population distribution among the rotational states may exhibit a superposition of local quasi-Boltzmannian distributions. Such artifacts were observed and explained for CO molecules in free jets[23] and sometimes interpreted erroneously as population inversions. The determination of the vibrational temperature for NH is a little hazardous, as pointed out before. The scatter in experimental data is very large, and a value of 7500 ± 2000 K is obtained along the axis.

The CN violet system leads to a much higher rotational temperature, 5000 ± 200 K along the axis (Fig. 9). A slight, but hardly significant, increasing tendency with distance can be observed. The vibrational temperatures from CN are found to be similar to those obtained with NH: 8000 ± 1000 K near the source, with again an increase with distance.

In Fig. 10 are reported the rotational temperatures of CH and N_2^+, as well as the vibrational temperature of CH, as a function of the methane concentration in nitrogen. For very low methane percentage (<0.5%), the N_2^+ rotational temperature is about 2500 K. This is in agreement with the rotational temperatures of CH and NH, as measured for the 1% methane mixture. For concentrations of methane higher than 1%, the rotational temperature of the nitrogen ion increases up to more than 4500 K, which is close to the rotational temperature of CN.

The atmosphere of Titan includes a percentage of argon, which is not yet very well known but might be as high as 25% (Ref. 24). It is observed that adding an amount of argon up to this percentage in the gas mixture has no significant influence on the measured spectra. This explains why the influence of argon has been disregarded along this work.

V. CO_2–N_2 Plasma

The present work, dealing with Mars atmosphere, is the following of a previous study carried out in 1995 at Laboratoire

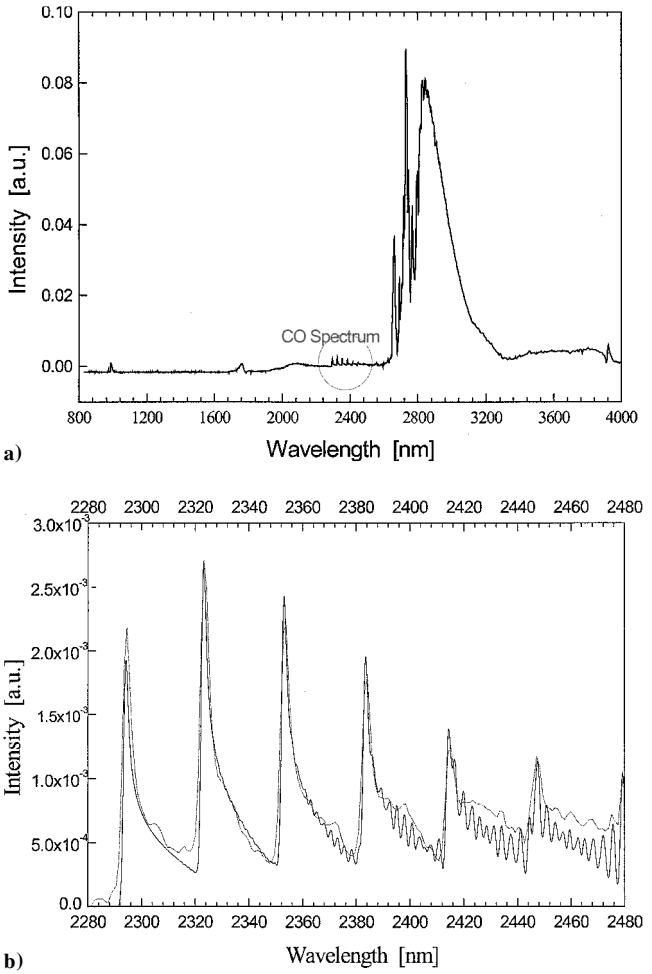

Fig. 11 IR spectrum of the CO_2 plasma, as obtained at CRMHT: a) general IR spectrum in the wavelength range 800–4000 nm; b) detailed view of the CO spectrum between 2280 and 2480 nm (pure CO_2). The simulated spectrum (——) is calculated with the temperatures T_v = 3500 K and T_r = 3500 K.

d'Aérothermique.[5] At this time the relative concentrations of the various chemical species inside the plasma jet were measured using a mass spectrometry technique. The present work is a first step in the measurement of the IR emission of plasmas containing CO_2. The main goal here is to analyze the IR emission of the CO molecule and to validate the simulation of the CO spectra for the $\Delta v = 2$ band.[25] These measurements are made with the FTIR experiment at the CRMHT laboratory (Figs. 2 and 4).

In Fig. 11a the flux emitted by a CO_2 plasma discharge at atmospheric pressure in the wavelength range 800–4000 nm is presented. The prominent feature of this spectrum is the large CO_2 flux emission with a superimposed structure corresponding to the H_2O molecule absorption lines. A much smaller structure can be observed around 2400 nm. This is the $\Delta v = 2$ band of the CO molecule, which is shown at a larger scale in Fig. 11b. On this figure is also shown the calculated spectrum obtained with rotational and vibrational temperatures equal to 3500 K and a wavelength spread of 1 nm at half maximum. The agreement between the experimental and simulated spectra is very good, for the intensity as well as for the band head wavelength locations.

VI. Conclusions

For the CO_2–N_2 plasma the emission in the visible and near UV wavelength range cannot be extracted from the background noise in the Laboratoire d'Aérothermique experimental conditions. IR emission is observed with the FTIR spectrometry experiment of CRMHT, corresponding to the $\Delta v = 2$ band of CO. IR measurements will also be performed in the near future with the arcjet experiment.

For the CH_4–N_2 plasma it is at first observed that the rotational as well as vibrational temperatures remain nearly constant along the plasma jet axis. This property is common to the different species, which are investigated here; but, the absolute values of the temperatures can be very different from one species to the other. Thus, the vibrational temperatures obtained for CN and NH are in concordance with each other and also in agreement with the electron temperature of 8000 K, as measured by an electrostatic probe. The vibrational temperature of CH is significantly lower, that is, only 3700 K. The rotational temperatures are high for CN and for N_2^+, both near 5000 K. Lower values of the rotational temperature are found for the two hydrides NH (2800 K) and CH (2500 K); these two temperatures can be considered as equal within the experimental error spread. This effect is not clearly understood because it seems to be in contradiction with the properties that can be deduced from the values of the moments of inertia, which are very different for the two groups because of the light H atom (rotational constant $B_e = 1.97$ and 1.65 for CN and N_2^+, respectively, 14 and 14.6 for NH and CH, respectively[18]).

The relative independence of temperatures with the axial distance is easily explained, at least for the vibrational temperature. The mean free path for vibrational relaxation in the conditions of the experiment is of the order of 1 cm. Furthermore, several tens of collisions are needed for relaxation. It is then likely that the temperatures are frozen in the expansion of the plasma and reflect directly the conditions inside the arc source. For rotational relaxation the situation is not so simple; the fact that the temperatures are lower should mean that relaxation is effective, and the fact that the temperatures are constant relative to distance that the relaxation occurred before the exit of the nozzle. Nevertheless, as just mentioned, the final rotational temperatures are different when the numbers of collisions necessary for relaxation are different. The limit of all of these rotational temperatures would be the translational temperature if the rotation-translation relaxation were complete. This will be checked by using a modified arc source where it will be possible to analyze the emission inside the divergent part of the nozzle where most of the relaxation process should take place.

References

[1] Auweter-Kurtz, M., Gölz, T., Habiger, H., Hammer, F., "100 kW Class Hydrogen Arcjet Thruster," *Proceedings of the 25th International Electric Propulsion Conference*, Electric Rocket Propulsion Society, Cleveland, OH, 1997, pp. 55–64.

[2] Deependran, B., Sujith, R. I., and Kurian, J., "Studies of Low-Density Freejets and Their Impingement Effects," *AIAA Journal*, Vol. 35, No. 9, 1997, pp. 1536–1542.

[3] Kuchi-Ishi, S., and Nishida, M., "Numerical Simulation of a Nonequilibrium Plasma Flow in a Nitrogen Arcjet Thruster Using a Three-Temperature Kinetic Model," *Proceedings of the 25th International Electric Propulsion Conference*, Electric Rocket Propulsion Society, Cleveland, OH, 1997, pp. 518–525.

[4] Röck, W., Auweter-Kurtz, M., Dabalà, P., Früholz, H., Habiger, H., and Laure, S., "Experimental Simulation of the Entry of Huygens into the Titan Atmosphere for the Thermal Protection Qualification," *Proceedings of the 44th Congress of the International Astronautical Federation*, Graz, Austria, 1993, pp. 1–10.

[5] Schönemann, A. T., Lago, V., and Dudeck, M., "Mass Spectrometry and Optical Spectroscopy in N_2–CO_2 and N_2–CH_4 Plasma Jets," *Journal of Thermophysics and Heat Transfer*, Vol. 10, No. 3, 1996, pp. 419–425.

[6] Beulens, J. J., Milojevic, D., Schram, D. C., and Valinga, P. M., "A Two-Dimensional Nonequilibrium Model of Cascaded Arc Plasma Flows," *Physics of Fluids B*, Vol. 3, No. 9, 1991, pp. 2548–2557.

[7] Megli, T. W., Krier, H., and Burton, R. L., "Plasmadynamics Model for Nonequilibrium Processes in N_2/H_2 Arcjets," *Journal of Thermophysics and Heat Transfer*, Vol. 10, No. 4, 1996, pp. 554–562.

[8] Scott, C. D., "Intrusive and Nonintrusive Measurements of Flow Properties in Arc Jets," *Proceedings of the Workshop on Hypersonic Flows for Reentry Problems*, INRIA-Sophia Antipolis and GAMNI-SMAI, Antibes, France, 1990, pp. 1–30.

[9] Meulenbroeks, R. F. G., Engeln, R. A. H., Beurskens, M. N. A., Paffen, R. M. J., van de Sanden, M. C. M., van der Mullen, J. A. M., and Schram, D. C., "The Argon-Hydrogen Expanding Plasma: Model and Experiments," *Plasma Sources Science and Technology*, Vol. 4, No. 1, 1995, pp. 74–85.

[10] Habiger, H. A., and Auweter-Kurtz, M., "Investigation of High-Enthalpy Air Plasma Flow with Electrostatic Probes," *Journal of Thermophysics and Heat Transfer*, Vol. 12, No. 2, 1998, pp. 198–205.

[11]Czernichowski, A., "Temperature Evaluation from the Partially Resolved 391 nm N_2^+ Band," *Journal of Physics D: Applied Physics*, Vol. 20, No. 5, 1987, pp. 559–564.

[12]Pellerin, S., Musiol, K., Motret, O., Pokrzywka, B., Cormier, J.-M., and Chapelle, J., "Application of the (0,0) Swan Band Spectrum for Temperature Measurements," *Journal of Physics D: Applied Physics*, Vol. 29, No. 11, 1996, pp. 2850–2865.

[13]Pellerin, S., Koulidiati, J., Motret, O., Musiol, K., de Graaf, M., Pokrzywka, B., and Chapelle, J., "Temperature Determination Using Molecular Spectra Simulation," *High Temperature Material Processes*, Vol. 1, No. 4, 1997, pp. 493–509.

[14]Pellerin, S., Musiol, K., Pokrzywka, B., Cormier, J.-M., and Chapelle, J., "Thermal Condition Control of an Arc Plasma CF_4 Reactor: Swan Band Spectrum for Temperature Measurements," *High Temperature Material Processes*, Vol. 1, No. 2, 1997, pp. 273–285.

[15]Scott, C. D., Blackwell, H. E., Arepalli, S., and Akundi, M. A., "Techniques for Estimating Rotational and Vibrational Temperature in Nitrogen Arcjet Flow," *Journal of Thermophysics and Heat Transfer*, Vol. 12, No. 4, 1998, pp. 457–464.

[16]Koulidiati, J., "Etude Spectroscopique des Molécules Carbonées Diatomiques. Application aux Diagnostics des Plasmas D'Hydrocarbures," Thesis, Univ. of Orléans, France, 1991.

[17]Laux, C. O., "Optical Diagnostics and Radiative Emission of Air Plasmas," High Temperature Gas Dynamics Lab., Report T-288, Stanford Univ., Aug. 1993.

[18]Huber, K. P., and Herzberg, G., "Constants of Diatomic Molecules," *Molecular Spectra and Molecular Structure*, Vol. 4, Van Nostrand, New York, 1979.

[19]Knowles, P., Werner, H. J., Hay, P., and Cartwright, D., "The $A^2\Pi$-$X^2\Sigma^+$ Red and $B^2\Sigma^+ - X^2\Sigma^+$ Violet Systems of CN Radical: Accurate Multireference Configuration Interaction Calculations of the Radiative Transition Probabilities," *Journal of Chemical Physics*, Vol. 89, No. 12, 1988, pp. 7334–7343.

[20]Ito, H., Ozaki, Y., Suzuki, K., Kondow, T., and Kuchitsu, K., "Analysis of the $B^2\Sigma^+ - A^2\Pi_i$ Perturbations in the CN ($B^2\Sigma^+ - X^2\Sigma^+$) Main Band System," *Journal of Molecular Spectroscopy*, Vol. 127, No. 1, 1988, pp. 283–303.

[21]Brazier, C., Ram, R., and Bernath, P., "Fourier Transform Spectroscopy of the $A^3\Pi - X^3\Sigma^-$ Transition of NH," *Journal of Molecular Spectroscopy*, Vol. 120, No. 2, 1986, pp. 381–402.

[22]Krupenie, P., and Lofthus, A., *Journal of Physical and Chemical Reference Data*, Vol. 6, 1977.

[23]Campargue, R., Gaveau, M. A., and Lebéhot, A., "Internal State Populations in Supersonic Free Jets and Molecular Beams," *Rarefied Gas Dynamics*, edited by H. Oguchi, Univ. of Tokyo Press, 1984, pp. 551–566.

[24]Nelson, H. F., Park, C., and Whiting, E. E., "Titan Atmospheric Composition by Hypervelocity Shock-Layer Analysis," *Journal of Thermophysics and Heat Transfer*, Vol. 5, No. 2, 1991, pp. 157–165.

[25]Piar, B., "Production des Molécules Excitées Vibrationnellement et Électroniquement par Pompage Laser. Analyse des États Formés," Thesis, Ecole Centrale, Châtenay-Malabry, France, 1993.